Journal of Magnetic Resonance 209 (2011) 167–173

Contents lists available at ScienceDirect

Journal of Magnetic Resonance

journal homepage: www.elsevier.com/locate/jmr

Construction and performance of an NMR tube with a sample cavity formed within magnetic susceptibility-matched glass

Mitsuhiro Takeda [a], Klaas Hallenga [b,1], Masahiro Shigezane [c], Markus Waelchli [d], Frank Löhr [e], John L. Markley [b], Masatsune Kainosho [a,f,*]

[a] Structural Biology Research Center, Graduate School of Science, Nagoya University, Furo-cho, Chikusa-ku, Nagoya 464-8602, Japan
[b] Department of Biochemistry, University of Wisconsin-Madison, 433 Babcock Drive, Madison, WI 53706-1544, USA
[c] Shigemi Inc., 2-4-5 Nakanosanno, Hachioji, 192-0042 Tokyo, Japan
[d] Bruker Biospin K.K., 3-9 Moriya-cho, Kanagawa-ku, Yokohama 221-0022, Japan
[e] Institute of Biophysical Chemistry, Centre for Biomolecular Magnetic Resonance, Goethe-University, Max-von-Laue-Str. 9, Biocentre, N230 1.OG, D-60438 Frankfurt am Main, Germany
[f] Center for Priority Areas, Tokyo Metropolitan University, 1-1 Minami-ohsawa, Hachioji, 192-0397 Tokyo, Japan

ARTICLE INFO

Article history:
Received 20 November 2010
Revised 6 January 2011
Available online 13 January 2011

Keywords:
Salt-tolerant NMR tube
Sample geometry alignment
Sample positioning holder
Susceptibility-matched glass

ABSTRACT

We describe the construction and performance of an NMR tube with a magnetic susceptibility matched sample cavity that confines the solution within the detection zone in the axial direction and in a quasi-rectangular region in the radial direction. The slot-like sample cavity provides both good sample volume efficiency and tolerance to sensitivity loss in the sample space. The signal-to-noise ratio per unit volume of the constructed tube was 2.2 times higher than that of a cylindrical tube of 5 mm outer diameter with a sample containing 300 mM NaCl at a static magnetic field of 14.1 T. Even the overall signal-to-noise ratio of the slot tube was 35% higher than that of the conventional 5 mm tube for a sample containing 300 mM NaCl. Similar improvements over existing sample tube geometries were obtained at 950 MHz. Moreover the temperature rise resulting from RF heating was found to be significantly lower for the slot tube even when compared to 3 and 4 mm outer diameter cylindrical tubes as measured in a 5 mm cryoprobe. A further advantage of this type of tube is that a sample cavity of any desired size and shape can be formed within a cylindrical tube for use in a single cryogenic probe.

1. Introduction

Over the past 20 years, the sensitivity of NMR signal detection has greatly increased owing to improved RF electronics and the advent of cryogenic probe technology [1–3]. In addition, on-going development of higher field magnets promises further improvements. However, ionic conductivity and dielectric losses with cryogenic probes at high magnetic field strengths severely limit the NMR sensitivity of aqueous solutions containing salt [4–6]. Optimization of sample tube design has recently begun to be appreciated as an approach to mitigating sensitivity losses.

When a cylindrical tube is placed in a Helmholtz probe, the magnitude of RF power dissipation varies widely within the sample space. In a radial cross-section of the tube, the power dissipation increases with distance from the center of the tube along a direction perpendicular to the B_1 field, resulting in the highest power dissipation at the edge regions [7]. Because the hot spots of RF power dissipation make a significant contribution to sensitivity loss and sample heating [8], the use of a cylindrical tube with smaller diameter or a tube in the shape of rectangle or oval reduces the effect [7,9,10]. For samples containing high salt, the signal-to-noise ratio (SNR) for a solution at a given concentration may not decrease appreciably, despite the fact that a smaller volume is used. For NMR analysis of quantity-limited samples, such sample tubes offer distinct advantages.

Here we describe the design and construction of a cylindrical sample tube containing a slot-shaped sample cavity fabricated from glass whose magnetic susceptibility matches to sample solvent (SM-glass). The susceptibility-matched material serves as an alternative to sample solvent and can be used to form the intended sample space [11]. In the slot tube design, SM-glass confines the sample within the detection zone in the axial direction as in a conventional Shigemi tube and two segment-shaped

* Corresponding author at: Center for Priority Areas, Tokyo Metropolitan University, 1-1 Minami-ohsawa, Hachioji 192-0397, Tokyo, Japan. Fax: +81 (0)42 677 4873.
E-mail address: kainosho@tmu.ac.jp (M. Kainosho).
[1] Present address: Stellingmolenlaan 12, 7241VZ Lochem, The Netherlands.

1090-7807/$ - see front matter © 2011 Elsevier Inc. All rights reserved.
doi:10.1016/j.jmr.2011.01.005

SM-glass pieces within the detection zone produce a quasi-rectangular shaped sample cavity. When the sample slot is properly oriented in an NMR probe. the design mitigates RF power dissipation in lossy samples [7]. We compare the performance of this tube to those of other types of sample tube. Because slot-shaped cavities of different size can be accommodated within a 5 mm cylinder, this basic design can be used to fabricate sample tubes for a variety of sample volumes.

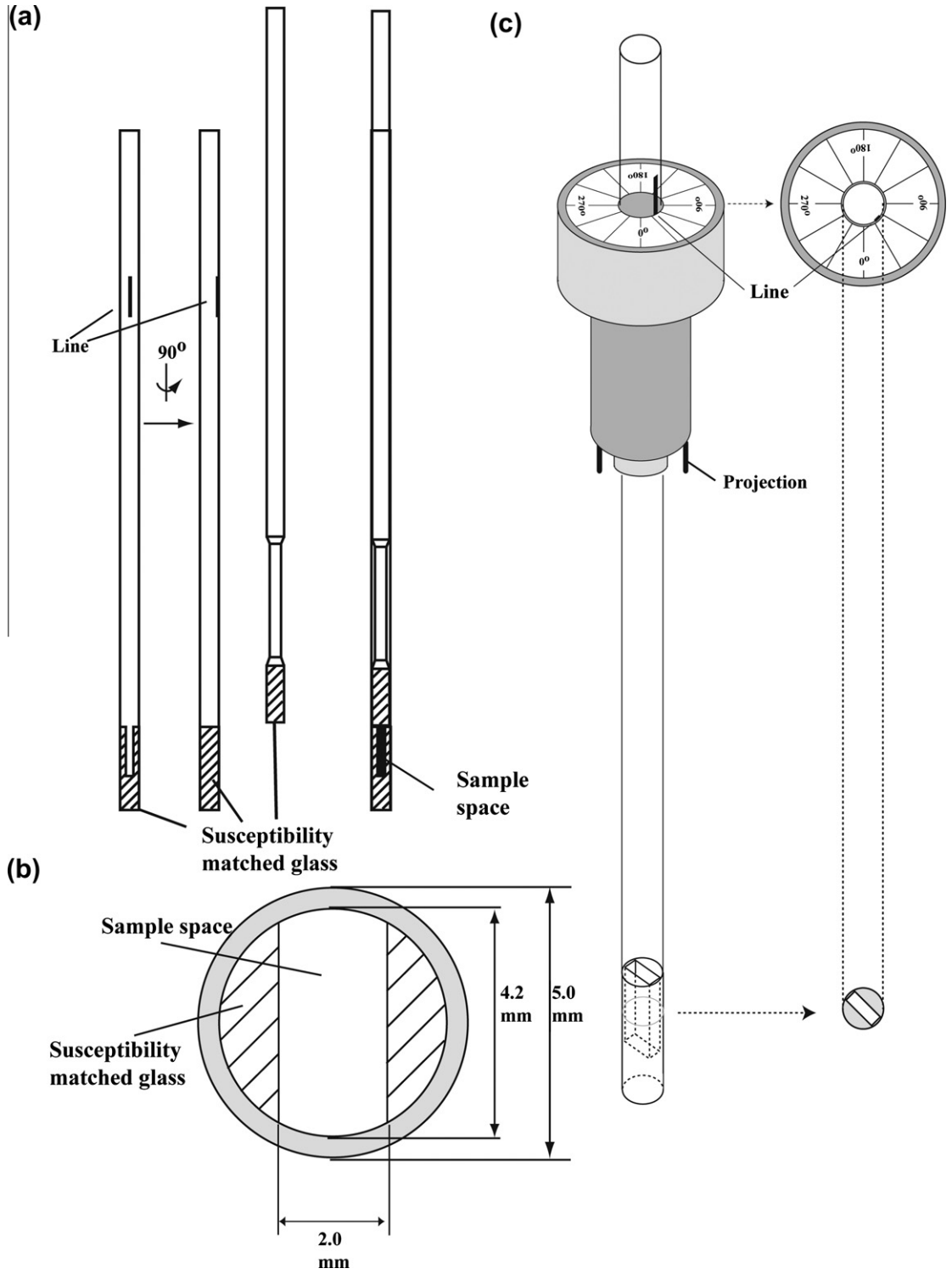

Fig. 1. Design of the slot tube. The slot tube is composed of an outer tube and a plunger (a). In the outer tube, the bottom beneath the sample space is filled with susceptibility-matched glass. Above it, two segment-shaped susceptibility-matched glass pieces create a quasi-rectangular sample space (b). The sample cavity is covered by the plunger made of susceptibility-matched glass. In the present study, the sample space was 2.0 mm in width and 20 mm in height, but these dimensions can be changed to alter the sample volume. A sample positioning unit (Bruker BioSpin) serves to orient the sample cavity in the NMR probe. The tailored sample holder has two projections in its bottom that insert into holes in the top of the probe. The top of the spinner is labeled with angle relative to the B_1 field and A line on the side of the tube marks the long axis of the slot, and the tube is rotated to align this line with the desired angle mark on the top of the sample holder (c).

2. Experimental

2.1. Construction of the slot tube

The slot tube (Fig. 1a) is composed of outer tube and a plunger as in microtubes manufactured by Shigemi Inc. The outer tube has an outside diameter of 5.0 mm, and the sample cavity is fabricated by using SM-glass in its bottom (Fig. 1b). The cross-section of the sample cavity in the radial direction has straight sides and arc shaped short ends and is approximately rectangular. The slot is 2 mm wide and 20 mm high. The plunger (Fig. 1a) has a SM-glass tip that forms the top of the sample cavity. The slot tubes will soon be commercially available from Shigemi Inc. A customized sample holder was initially fabricated from a standard 5-mm spinner by the mechanical workshop at Goethe University (Frankfurt) using a Bruker shaped-tube sample holder as a guideline and later by Bruker BioSpin, with pins projecting from its bottom that engage the sample positioning unit in the probe (Bruker BioSpin); the two projections fit into two holes located on the top of the NMR probe. The slot is oriented at the desired angle by aligning a line on the lateral surface with markings on the top of the tube holder (Fig. 1b and c).

2.2. Sample preparation

A sample solution was prepared that contained 0.3 mM [U-^{13}C, ^{15}N]-chlorella ubiquitin (Chlorella Industry Co. Ltd., Tokyo, Japan) in 10 mM sodium phosphate (pH 6.6) in H_2O/D_2O = 90/10. A similar sample containing 0.3 mM of [U-^{13}C, ^{15}N]-chlorella ubiquitin and 300 mM NaCl was used in comparing the performance of cylindrical microtubes (Shigemi) with different diameters: 3 mm outer diameter (2.5 mm i.d.) and 4 mm outer diameter (3.2 mm i.d.). For both microtubes, the height of the solution space was adjusted to 20 mm. A set of four ubiquitin samples was prepared containing 0.3 mM protein in H_2O/D_2O = 90/10 with NaCl concentrations of 0, 100, 200 and 300 mM. These solutions were used in comparing the performance of three NMR tubes: the slot tube, a 5 mm o.d. microtube (Shigemi), and an oval-shaped tube (Bruker BioSpin). The height of the solution space was adjusted to 20 mm by inserting the plunger in the microtube and to 40 mm in the oval-shaped tube.

2.3. NMR experiments and analysis

NMR experiments were performed on a DRX600 spectrometer (Bruker BioSpin; 600.2 MHz for ^{1}H) or a Av950 spectrometer (Bruker BioSpin; 950.1 MHz for ^{1}H) at 25 °C. Both spectrometers were equipped with a TCI cryogenic probe with a sample positioning unit (Bruker BioSpin): two holes on the head of probe accommodate corresponding projections underneath the customized sample holder (Fig. 1c). In the ^{1}H 1D NMR experiments, the water peak was suppressed by pre-saturation with a RF transmitter output of 0.4 W. In TROSY-HSQC experiments [12], a flip-back pulse sequence was used to achieve water peak suppression. The ^{1}H pulse length was determined for each experimental condition, and thus the ^{1}H pulse excitation profile differed slightly among the experiments. The effects of pulse imperfections on the intensities of signals far from the carrier frequency were not considered in data analysis. In the experiments at 14.1 T, the data size and spectral width were 512 (256) (t_1) × 1024 (512) (t_2) (complex) points and 2100 Hz (ω_1, ^{15}N) × 9600 Hz (ω_2, ^{1}H), respectively, and the number of scans/FID was 2. The ^{15}N and ^{1}H carrier frequencies were 117.5 ppm and 4.7 ppm, respectively. The repetition time was 1 s. In the experiments at 22.3 T, the data size and spectral width were 512 (t_1) × 2048 (t_2) points and 2100 Hz (ω_1, ^{15}N) × 7200 Hz (ω_2, ^{1}H), respectively, and the number of scans/FID was 2. The ^{15}N and ^{1}H carrier frequencies were 117.5 ppm and 4.7 ppm, respectively. The repetition time was 1 s. The data were processed by TopSpin software (Bruker BioSpin). The data sets were zero-filled in the direct and indirect dimensions to 4096 (F1) × 1024 (F2), and a QSINE window with SSB = 2 was applied in both F1 and F2 directions. The ^{1}H–15N TROSY-HSQC peak patterns obtained with the slot tube and cylindrical tubes were identical for samples at a given salt concentration, but the positions of most peaks exhibited a small dependence on salt concentration, probably due to a subtle alteration of conformation and/or dynamics. Peak intensities were evaluated for six residues in the Lys27–Lys32 α-helix region from 1D slices in the ^{1}H dimension at each salt concentration. The noise level was evaluated from the spectral region from 3 to −1 ppm, in which no peak is present. The "SINOCAL" command in TopSpin software (Bruker BioSpin) was used to determine the SNR.

RF sample heating for the slot tube and the 3, 4, and 5 mm o.d. mirotubes (20 mm sample height in each case) was evaluated by monitoring the increase in sample temperature of 99% D_2O water containing 1 mM DSS and 300 mM NaCl (pH 4.8) following continuous wave irradiation with a RF transmitter output power of 0.4 W at ^{1}H frequency of 30 ppm for variable times. The experiments were performed on a DRX600 NMR spectrometer equipped with a TCI cryogenic probe at 25 °C. Following the application of 32 dummy pulses, the ^{1}H 1D spectrum was acquired as two transients. The increase in sample temperature was determined from the chemical shift difference between the HDO peak and the methyl peaks of 4,4-dimethyl-4-silapentane-1-sulfonic acid (DSS) [13] according to $\Delta T = 86.2 \times \Delta\delta$, where ΔT is the increase in temperature in Kelvin unit and $\Delta\delta$ is the decrease in chemical shift difference between HDO and methyl peaks in ppm units.

3. Results and discussion

3.1. Basic performance of the slot tube

Initially, we checked whether the sample tube can be orientated at desired angles in an NMR probe on the basis of the orientation dependence of the $\pi/2$ pulse length [14]. The $\pi/2$ pulse length

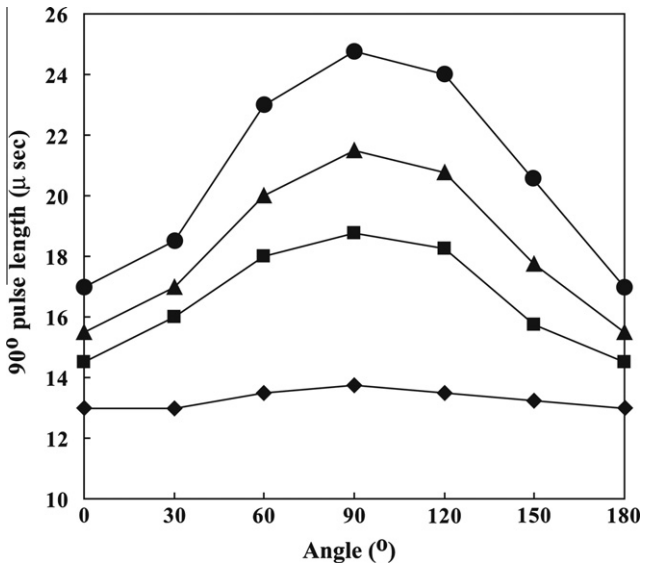

Fig. 2. Measured $\pi/2$ pulse lengths for solutions containing different concentrations of NaCl and different orientations of the sample cavity in the slot tube. Under fixed RF transmitter power (31.6 W), $\pi/2$ pulse lengths were determined for solutions containing 0 mM (♦), 100 mM (■), 200 mM (▲) or 300 mM (●) NaCl at 30° intervals on a DRX600 MHz NMR spectrometer. The sample buffer contained 10 mM sodium phosphate (pH 6.6). An angle of 0 corresponds to placing the tube such that the long axis of the slot is parallel to the B_1 field. For comparison, the $\pi/2$ pulse lengths for a 5 mm o.d. microtube were as follows: 0 mM NaCl: 14 μs; 100 mM NaCl: 20.5 μs; 200 mM NaCl: 24 μs; 300 mM NaCl: 28 μs.

should be minimized when the long axis of sample cross-section is aligned with the direction of the B_1 field, and maximized when it is perpendicular. The observed profile of the $\pi/2$ pulse length was reproducibly consistent with this expectation (Fig. 2), and this approach was used to orient the slot tube at the desired angle in the NMR probe.

As a next step, we tested whether fine quality NMR spectra can be acquired with the slot tube under practical conditions for protein NMR including automatic shimming [15]. Overall, the quality of ^{1}H 1D NMR, 2D ^{1}H–15N, and 2D ^{1}H–13C spectra of a sample in a the slot tube were nearly identical to those from the sample in a conventional Shigemi 5 mm microtube (Fig. 3).

3.2. Comparison of the salt tolerance of the slot tube to that of other types of tubes

We compared the salt tolerance of the slot tube with that of a 5 mm microtube (Shigemi) and an oval-shaped tube (Bruker BioSpin) by measuring SNR of peaks in ^{1}H–15N TROSY-HSQC spectra of 0.3 mM [U-^{13}C, ^{15}N]-ubiquitin samples at NaCl concentrations of 0, 100, 200 and 300 mM and at static magnetic fields of 14.1 (Table 1) and 22.3 T (Table 2).

In the absence of added salt, the highest SNR was achieved with the 5 mm microtube. However, at the highest salt concentration (300 mM), a concentration frequently required to solubilize pro-

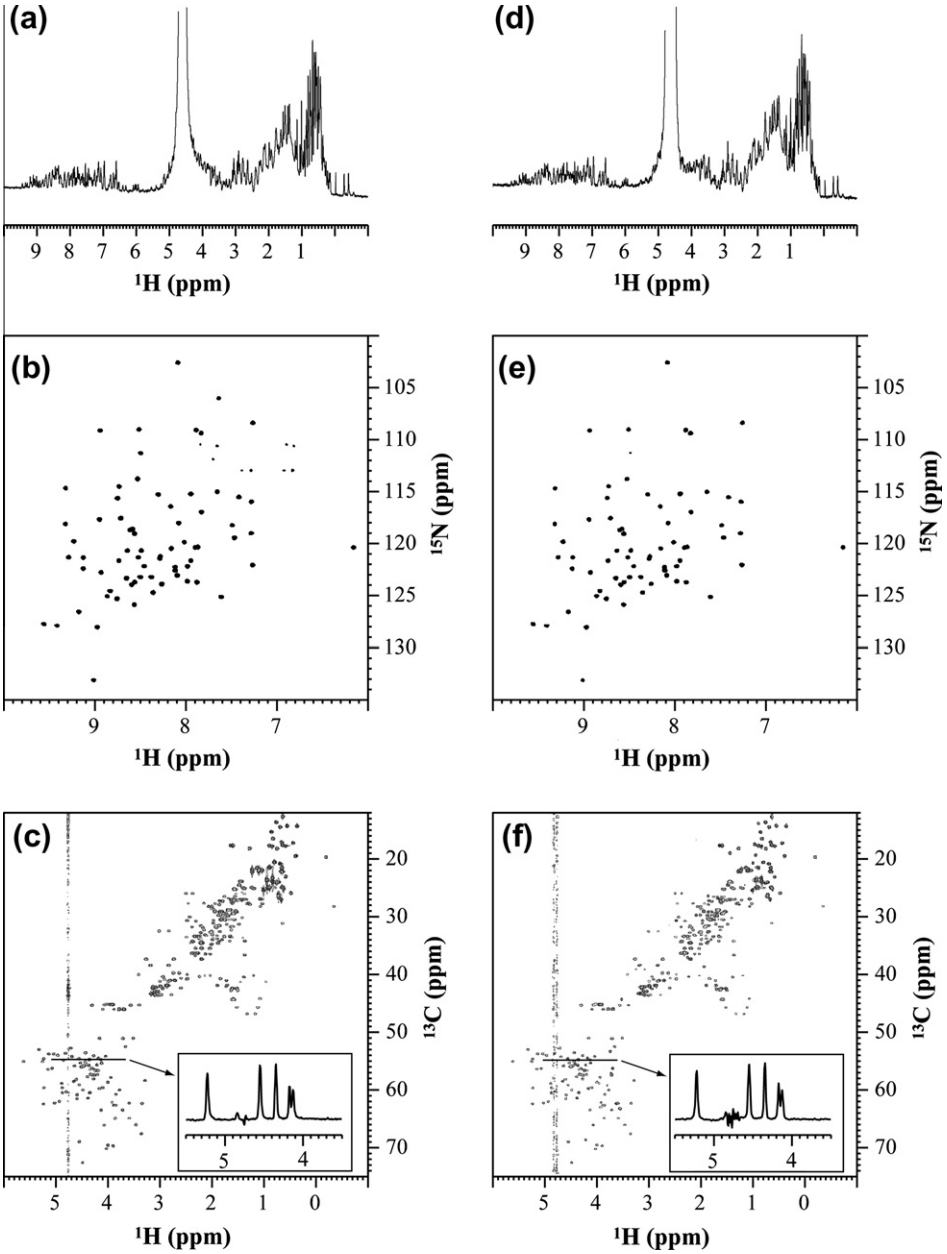

Fig. 3. Comparison of NMR spectra acquired with the slot tube and the 5 mm microtube. NMR spectra of 0.3 mM of [U–^{13}C/^{15}N]-ubiquitin containing 10 mM sodium phosphate (pH 6.6) in the 5 mm microtube (a–c) and the slot tube (d–f). All these data were acquired on an Avance 950 NMR spectrometer (22.3 T) equipped with a TCI cryogenic probe at 25 °C. (a and d) ^{1}H 1D experiment with the water peak was suppressed by continuous wave irradiation at a fixed RF transmitter power. (b and e) ^{1}H–^{15}N TROSY-HSQC experiments with a water flip-back pulse. (NS = 2; 512 (F1) × 1536 (F2) with 3400 Hz (ω_1, ^{15}N) × 11,400 Hz (ω_2, ^{1}H)) (c and f) ^{1}H–^{13}C constant time HSQC experiments (NS = 2; 916 (F1) × 1536 (F2) with 16,900 Hz (ω_1, ^{13}C) × 11,400 Hz (ω_2, ^{1}H)). The constant time was 26.6 ms and both positive and negative peaks are displayed. To clarify the relative intensity of the remaining water to the protein signals, the 1D slice of the experiments at ^{13}C chemical shift of 55 ppm are displayed in the inset. The experimental conditions were identical between the 5 mm microtube and the slot tube except for the ^{1}H pulse length.

Table 1
Summary of results at different salt concentrations and tube geometries at 14.1 T (^{1}H frequency of 600 MHz).

NMR tube	Sample volume (μl)	Concentration of NaCl (mM)	$\pi/2$ Pulse length (μs)	Observed SNR	SNR per unit volume (ml)
Slot tube	170	0	12.7	74 ± 6	435 ± 34
		100	13.9	63 ± 6	371 ± 34
		200	15.1	55 ± 7	320 ± 38
		300	15.8	46 ± 4	273 ± 25
5 mm o.d. microtube	280	0	13.3	123 ± 10	438 ± 35
		100	19.5	58 ± 5	206 ± 17
		200	23.0	44 ± 4	157 ± 15
		300	27.3	34 ± 3	123 ± 9
Oval-shaped tube	380	0	12.4	100 ± 6	263 ± 16
		100	14.2	61 ± 4	161 ± 11
		200	15.5	50 ± 3	131 ± 7
		300	16.9	44 ± 3	115 ± 7

Table 2
Summary of results at different salt concentrations and tube geometries at 22.3 T (^{1}H frequency of 950 MHz).

NMR tube	Solvent volume (μl)	Concentration of NaCl (mM)	$\pi/2$ Pulse length (μs)	Observed SNR	SNR per unit volume (ml)
Slot tube	170	0	8.7	125 ± 8	735 ± 49
		100	10.0	91 ± 7	534 ± 43
		200	10.8	88 ± 6	517 ± 35
		300	11.6	78 ± 7	458 ± 41
5 mm o.d. microtube	280	0	10.1	155 ± 16	554 ± 59
		100	14.3	87 ± 9	312 ± 32
		200	17.3	72 ± 7	257 ± 26
		300	20.0	56 ± 5	199 ± 16
Oval-shaped tube	380	0	8.8	117 ± 13	308 ± 35
		100	10.0	87 ± 7	229 ± 19
		200	10.9	74 ± 7	196 ± 18
		300	12.0	62 ± 4	164 ± 11

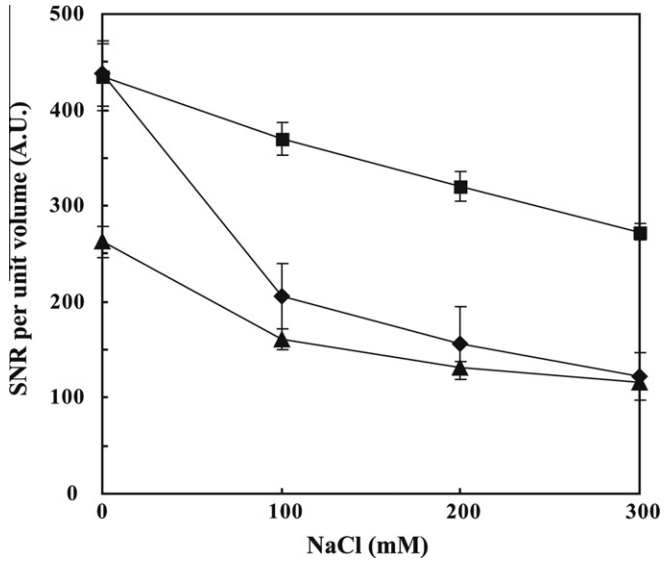

Fig. 4. SNR per unit volume in different tubes and salt concentrations. The SNR per unit volume for data acquired at 14.1 T (600 MHz ^{1}H) evaluated for the 0.3 mM ubiquitin samples in the slot tube (■), 5 mm o.d. microtube (♦), and oval-shaped tube (▲) at different salt concentrations.

teins, all three tube designs achieved comparable SNR values, with the slot tube and oval-shaped tube slightly outperforming the 5 mm microtube at both 600 MHz (Table 1) and 950 MHz (Table 2).

In general, proteins and other biomolecules are quite expensive to produce, particularly when they are labeled uniformly or selectively with stable isotopes (^{2}H, ^{13}C, and or ^{15}N). In addition, these biomolecules frequently have limited solubility and require the addition of salt to achieve solubility and stability. Thus the SNR per unit volume with samples of equal concentration is the most important criterion for comparison. Comparison of the SNR per unit volume values demonstrates the clear advantages of the slot tube design over the two alternatives at all salt concentrations and particularly at high salt and at high magnetic field. For example, at 600 MHz the SNR per unit volume for the protein solution containing 300 mM NaCl was over two times higher than for that of the other designs (Table 1) while at 950 MHz it was over two times higher than that for the 5 mm microtube and nearly three times higher than that of the oval-shaped tube at 950 MHz (Table 2).

As shown in Fig. 4, the gradient of the decrease in the SNR per unit volume with increasing salt concentration was gentle for the slot tube and oval-shaped tube but much steeper for the 5 mm microtube. Similar results are shown by the salt dependence of the increase in the $\pi/2$ pulse length (Table 1). These results demonstrate that the shape of the slot tube, like that of the oval tube, successfully mitigate sensitivity losses arising from the ionic conductivity.

The improvement of SNR of the slot tube over the 5 mm microtube at 22.3 T was nearly identical to that at 14.1 T within experimental error (Table 3). According to the report by Horiuchi and coworkers, the dielectric conductivity for water at 930 MHz is equivalent to the ionic conductivity of solution containing as little as 20 mM NaCl. (See Fig. 3 of Ref. [6]). Because dielectric losses increase drastically with increasing magnetic field over 1 GHz, the contribution of the dielectric tolerance of the slot tube should become more apparent at these higher fields. Also, dielectric losses increase markedly with decreasing temperature for aqueous solutions such that at 5 °C they become equivalent to those of 50 mM NaCl at 900 MHz.

A current alternative to a shaped tube is to place the sample in cylindrical tube of smaller diameter. We have compared SNR with the protein sample containing 300 mM NaCl achieved with a 3 mm microtube (Shigemi), a 4 mm microtube (Shigemi), and the slot tube (Table 4). The SNR per unit volume is best for the 3 mm microtube (321) followed by that for the slot tube (273). However, if the sample quantity is not limiting, the slot tube provides the overall best SNR.

Table 3
Sensitivity gain at static magnetic fields of 14.1 T and 22.3 T.

NaCl (mM)	SNR ratio (slot tube / microtube)	
	14.1 T (^{1}H: 600 MHz)	22.3 T (^{1}H: 950 MHz)
0	1.0 ± 0.2	1.3 ± 0.2
100	1.8 ± 0.2	1.7 ± 0.3
200	2.0 ± 0.2	1.9 ± 0.4
300	2.2 ± 0.4	2.3 ± 0.4

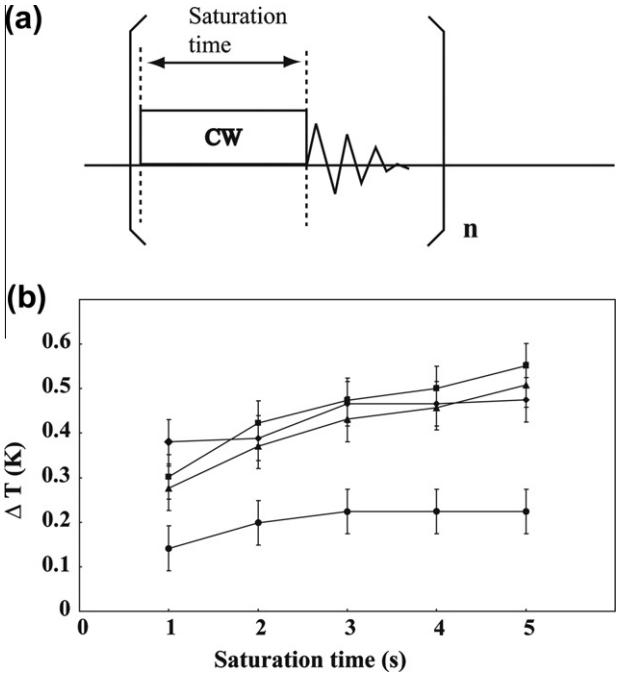

Fig. 5. Evaluation of the sample heating in different tubes: (a) pulse sequence employed to evaluate the heating of a 99% D_2O water sample containing 1 mM DSS and 300 mM NaCl (pH 4.8). The experiments were performed using a DRX600 NMR spectrometer equipped with a TCI cryogenic probe regulated at 25 °C. Presaturation was carried out by continuous wave irradiation at a transmitter output of 0.4 W. Following the application of 32 dummy pulses, the ^{1}H 1D spectrum was acquired in two transients. The increase of the sample temperature was measured from the chemical shift difference between the HDO peak and the methyl peaks of DSS and (b) results for the slot tube (●), 3 mm o.d. microtube (▲), 4 mm o.d. microtube (■), 5 mm o.d. microtube (♦).

To evaluate the influence of sample tube design on sample heating, we compared the performance of the slot tube with that of three microtubes of 3, 4 and 5 mm outer diameters (Fig. 5). The slot tube showed a much lower heating over time and reached a steady state plateau earlier than the other designs. Because the heat conductivity of glass is larger than that of surrounding air, sample heat appears to be dissipated more efficiently by the slot tube.

This can be understood by considering the following four factors:

1. The amount of RF dissipation in high conductivity samples, which is comparable for the Slot tube and the 3 mm tube but higher for the 5 and 4 mm tubes. This follows from the $\pi/2$ pulse lengths given in Tables 1, 2 and 4.
2. The ratio of glass surface per unit volume. This can be calculated by dividing the circumference of the cross-section for each tube by its relative volume as shown in Table 5. In this aspect the Slot tube and the 3 mm tube have the highest ratio. The 4 and 5 mm tube have respectively about 15% and 35% lower surface-to-volume ratios.
3. The larger thermal conductivity (about 70%) of glass as compared to the solvent H2O. This puts the slot tube again at an advantage over the 5 and 4 mm tubes.
4. The difference in airflow patterns between 5, 4 and 3 mm o.d. tubes when tested in a probe designed for 5 mm o.d. (or oval tubes). The cooling by air is most efficient in this configuration for the Slot tube and the 5 mm cylindrical tube. The heat exchange will be least efficient for the 3 mm tube and somewhat better for the 4 mm tube.

4. Conclusion

The slot tube described here exhibits practical advantages over alternative tube designs in terms of SNR per unit volume and minimization of sample heating, particularly for samples containing high salt concentrations and data collected at high fields. Use of the slot tube can minimize the quantity and hence the cost of biomolecular samples. The higher SNR achieved can reduce the required data collection time and enable data collection with samples that degrade over time. The slot tube can readily be introduced into normal laboratories at low cost, particularly when the probe is equipped with a sample positioning unit. Finally, the slot tube design likely will exhibit further advantages as NMR systems are developed that operate at still higher static magnetic fields.

Table 4
Summary of S/N at other type of tube geometries at ^{1}H frequency of 600 MHz.

NMR tube	Solvent volume (μl)	Concentration of NaCl (mM)	$\pi/2$ Pulse length (μs)	Total SNR	SNR per unit volume
Slot tube	170	300	15.8	46 ± 4	273 ± 25
4 mm o.d. microtube	163	300	18.9	32 ± 2	197 ± 12
3 mm o.d. microtube	98	300	15.0	31 ± 2	321 ± 21

Data are for 0.3 mM of [U-^{13}C, 15 N]-ubiquitin sample at 600 MHz.

Table 5
Comparison of relative glass–liquid surface/volume ratio.

NMR tube	Solvent volume (μl)	Relative volume	Length of glass–liquid cross-section (mm)	Rel. glass–liquid surface/volume ratio
Slot tube	170	0.60	12.2	20.3
4 mm o.d. microtube	163	0.58	10.05	17.3

Acknowledgments

This work was supported in part by Targeted Protein Research Program (MEXT) to M.K., and a Grant-in-Aid for Young Scientist (B) (21770110) to M.T. We thank Prof. Volker Dötsch, Institute of Biophysical Chemistry and Center of Biological Magnetic Resonance, Goethe-University, for his kind help in collecting the NMR data at ^{1}H frequency of 950 MHz. Mr. Klaus Müller (Goethe University) is gratefully acknowledged for manufacturing the prototype sample holder for slotted NMR tubes. J.L.M. and K. H. were supported by US NIH Grant P41 RR02301.

References

[1] P. Styles, N.F. Soffe, C.A. Scott, An improved cryogenically cooled probe for high-resolution NMR, J. Magn. Reson. 84 (1989) 376–378.
[2] M. Jerosch-Herold, R.K. Kirschman, Potential benefits of a cryogenically cooled NMR probe for room-temperature samples, J. Magn. Reson. 85 (1989) 141–146.
[3] H. Kovacs, D. Moskau, M. Spraul, Cryogenically cooled probes—a leap in NMR technology, Prog. NMR Spectrosc. 46 (2005) 131–155.
[4] D.G. Gadian, F.N.H. Robinson, Radiofrequency losses in NMR experiments on electrically conducting samples, J. Magn. Reson. 34 (1979) 449–455.
[5] A.E. Kelly, H.D. Ou, R. Withers, V. Dötsch, Low-conductivity buffers for high-sensitivity NMR measurements, J. Am. Chem. Soc. 124 (2002) 12013–12019.
[6] T. Horiuchi, M. Takahashi, J. Kikuchi, S. Yokoyama, H, Maeda, Effect of dielectric properties of solvents on the quality factor for a beyond 900 MHz cryogenic probe model, J. Magn. Reson. 174 (2005) 34–42.
[7] T.M. de Swiet, Optimal electric fields for different sample shapes in high resolution NMR spectroscopy, J. Magn. Reson. 174 (2005) 331–334.
[8] A.C. Wang, A. Bax, Minimizing the effects of radio-frequency heating in multidimensional NMR experiments, J. Biomol. NMR 3 (1993) 715–720.
[9] L.C. Robosky1, M.D. Reily1, D. Avizonis, Improving NMR sensitivity by use of salt-tolerant cryogenically cooled probes, Anal. Bioanal. Chem. 387 (2007) 529–532.
[10] M.W. Voehler, G. Collier, J.K. Young, M.P. Stone, M.W. Germann, Performance of cryogenic probes as a function of ionic strength and sample tube geometry, J. Magn. Reson. 183 (2006) 102–109.
[11] R. Kc, Y.N. Gowda, D. Diukovic, I.D. Henry, G.H. Park, D. Raftery, Susceptibility-matched plugs for microcoil NMR probes, J. Magn. Reson. 205 (2010) 63–68.
[12] K. Pervushin, R. Riek, G. Wider, K. Wüthrich, Attenuated T_2 relaxation by mutual cancellation of dipole–dipole coupling and chemical shift anisotropy indicates an avenue to NMR structures of very large biological macromolecules in solution, Proc. Natl. Acad. Sci. USA 94 (1997) 12366–12371.
[13] D.S. Wishart, B.D. Sykes, Chemical shifts as a tool for structure determination, Methods Enzymol. 239 (1994) 363–392.
[14] D.I. Hoult, R.E. Richards, The signal-to-noise ratio of the nuclear magnetic resonance experiment, J. Magn. Reson. 24 (1976) 71–85.
[15] M. Weiger, T. Speck, M. Fey, Gradient shimming with spectrum optimization, J. Magn. Reson. 182 (2006) 38–48.